Extensive tests on the application of reverse Monte Carlo modelling to single-crystal neutron diffuse scattering from ice Ih

1997 J. Phys.: Condens. Matter 9 5145

(http://iopscience.iop.org/0953-8984/9/24/013)

J. Phys.: Condens. Matter **9** (1997) 5145–5156. Printed in the UK PII: S0953-8984(97)82101-7

Extensive tests on the application of reverse Monte Carlo modelling to single-crystal neutron diffuse scattering from ice Ih

M N Beverley and V M Nield

Physics Laboratory, University of Kent, Canterbury, Kent CT2 7NR, UK

Received 24 February 1997, in final form 22 April 1997

Abstract. Single-crystal diffuse scattering contains a great deal of information on instantaneous atomic positions, and hence on local correlations, static disorder and thermal motion of the atoms. In an attempt to extract as much of this information as possible, a reverse Monte Carlo technique, RMCX, was specially developed. The present paper reports the results of some tests on this technique. It has been found that the results are strongly dependent on the initial molecular geometry and the $\boldsymbol{Q}$-resolution of the data.

1. Introduction

Bragg scattering contains information on the long-range order in a crystal, and hence its interpretation yields accurate coordinates for the average atomic sites together with the corresponding thermal ellipsoids. However information regarding deviations from the average cannot be extracted directly from this type of scattering. Diffuse scattering originates from thermal motions and from static disorder and so contains information complementary to that from Bragg scattering. In previous papers a method of analysing single-crystal diffuse scattering based on the reverse Monte Carlo technique was discussed (Nield 1995, Nield *et al* 1995). The results from its detailed application to the normal form of ice, ice Ih, were appreciably different from accepted values (Nield and Whitworth 1995, which will hereafter be referred to as paper I). Some attempts were made to decrease the mean square displacements by adding constraints on the range of allowed O–D distances and D–O–D angles, but these proved largely unsuccessful (Nield 1995, Beverley and Nield 1997). In an attempt to understand the limitations of the RMCX technique, and to try and alleviate them, various trials have been performed and these form the subject of this paper. They include the use of a modified form, RMCXMOLS, in which the molecule is kept rigid. Details of RMCXMOLS and all the performed modelling runs are the subject of sections 2 and 3. The results are discussed and compared to those from other techniques and from paper I in section 4.

2. Reverse Monte Carlo modelling of ice

The reverse Monte Carlo (RMC) modelling technique was primarily developed to extract short-range structural information from neutron diffraction data of liquids and amorphous materials (McGreevy and Pusztai 1988). Currently the procedure allows the interpretation

0953-8984/97/245145+12$19.50

of neutron, x-ray and extended x-ray fine structure (EXAFS) scattering data from various systems (McGreevy and Howe 1992). This is achieved by producing an ensemble of atoms which yields scattering comparable with that measured experimentally.

A recent investigation of the single-crystal diffuse neutron scattering from deuterated ice Ih was performed by Li *et al* (1994). In ice Ih the oxygen atoms occupy a regular tetrahedral network, with the hydrogen atoms disordered over four sites surrounding each oxygen, but complying with the rules of Bernal and Fowler (1933). These require each oxygen to be covalently bonded to two hydrogens, and only one hydrogen to be located between neighbouring oxygens. This leads to strong diffuse scattering. The scattering was measured on SXD at ISIS (Rutherford Appleton Laboratory, UK) over a very large volume of reciprocal space, corrected, normalized and binned dependent on the configuration size (see equation (1) below). To analyse these data the RMC method was adapted, enabling the simultaneous modelling of single-crystal diffuse scattering in several crystallographic planes. This technique, known as RMCX, minimizes the difference between the experimental scattering and that from a configuration of atoms for each plane concurrently. For a complete treatment of the RMCX technique the reader is referred to Nield *et al* (1995). A further development is RMCXMOLS, in which the molecule is kept rigid. The algorithms are described and compared below.

(i) An initial configuration is produced. In the present case this consisted of a finite repetition of the orthorhombic unit cell (chosen over the more usual hexagonal one for ice for ease of modelling), with the hydrogen atoms positioned so as to obey the Bernal–Fowler rules (Li *et al* 1994). The molecules contained within the the unit cell are described in terms of the individual atomic coordinates when using RMCX, whereas for RMCXMOLS the molecule is described by two sets of parameters: its position, given by the oxygen coordinates, and its orientation, which is denoted by three Euler angles. The fulfillment of periodic boundary conditions requires the spacing of the data $\boldsymbol{Q}$ points to be related to the number of unit cells by

$$\boldsymbol{Q} = 2\pi \left(\frac{h'}{an_a}, \frac{k'}{bn_b}, \frac{l'}{cn_c} \right) \tag{1}$$

where a, b, c are the lattice parameters for a configuration with n_a, n_b, n_c unit cells in the Cartesian directions and h', k' and l' are integers.

(ii) The coherent scattering from the starting configuration is calculated.

(iii) The random displacement of an atom/molecule is performed. In RMCX an atom chosen at random is displaced in a random direction. The magnitude of the move is also random although limited by the user. For the RMCXMOLS method, a molecule is selected at random and is both displaced and rotated at random up to user specified amounts.

(iv) The distances of the moved particles from all other particles are checked to ensure that the move has not produced an unphysical situation.

(v) The coherent scattering of the new ensemble is calculated and compared to that measured experimentally. The move is accepted if the fit to the experimental data has improved. The move is also accepted with a certain probability if the fit to the data has deteriorated.

(vi) The procedure is repeated from step (iii) until the fit has converged.

3. Calculations and results

In paper I the configuration consisted of a $6 \times 6 \times 6$ repetition of an eight-molecule orthorhombic unit cell of dimensions $a = 4.498$ Å, $b = 2a \sin 60^\circ$, $c = 7.323$ Å, with the deuterium atoms obeying the Bernal–Fowler rules. The O–D lengths and D–O–D angles

were 0.975 Å and 107.0°, respectively. RMCX was used in the fitting of five experimental planes of data (the 0 k l and its equivalent h h l, the h 0 l and its equivalent h 3h l and the h k 0 plane) measured by Li *et al* (1994). The results of paper I are reproduced in table 1, where the statistical error was obtained by averaging over twenty individual configurations. Figure 1 describes the notation used in the table. In the present study the same experimental data were modelled, but both $6 \times 6 \times 6$ and $10 \times 10 \times 10$ unit cell configurations were used, and so they were binned differently in the two cases (equation (1)). This is equivalent to using data with different $\boldsymbol{Q}$-resolution in the two cases. In all $10 \times 10 \times 10$ cases points within a cube of 0.1 reciprocal lattice units from a Bragg peak were removed, as they contained some intensity from the tails of the Bragg peaks.

Table 1. Results obtained in paper I from modelling with RMCX only using a $6 \times 6 \times 6$ configuration. The second and third columns give, respectively, the mean and full-width-at-half-maximum (FWHM) values for these quantities. All distances are given in Å and all angles in degrees.

	Mean	FWHM
O–O″	2.768(2)	0.36
O–O′	2.743(5)	0.36
O–D_2	0.999(2)	0.35
O–D_1	0.987(4)	0.35
O- -D''_2	1.801(3)	0.35
O- -D'_1	1.787(6)	0.35
D_2-D_3	1.577(6)	0.34
D_2-D_2	1.579(5)	0.34
D_2- -D''_3	2.318(1)	0.32
D_2- -D'_1	2.313(1)	0.32
O″–O–O″	109.1(1)	11
O′–O–O″	109.5(1)	11
D_2–O–D_3	105.6(4)	30
D_2–O–D_1	106.1(5)	30
O–D_2- -O″	164.3(3)	23
O–D_1- -O′	164.4(5)	23

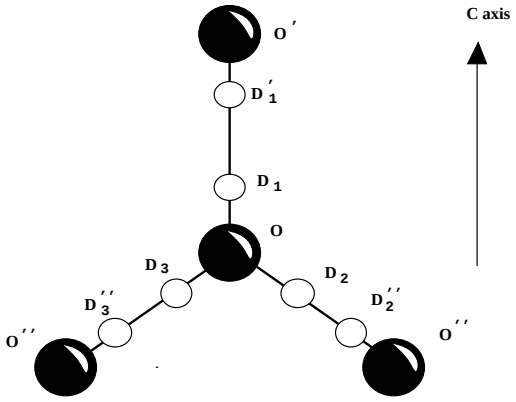

Figure 1. An illustration of the notation used in the text and tables for the various inter-atomic distances and angles in ice.

Two different modelling approaches were used. In the first RMCXMOLS was applied, keeping the molecule completely rigid, and only once the fit was as good as possible was RMCX applied, allowing relaxation of the molecule. In the second procedure RMCX was applied throughout. In both cases different molecular geometries were used, and the amount of rotation was varied (RMCXMOLS only). The starting configurations were also altered, with either the O–O distances oblique and along the *c*-axis equal or all O–O–O angles equal (and hence O–O′ not equal to O–O″). In this study the closest approaches for two atomic centres were generally 2.3, 0.9 and 1.4 Å for the O–O, O–D and D–D distances respectively. These are larger than those used in paper I, where the same parameters were 2.3, 0.5 and 1.0 Å, respectively. The move sizes allowed during RMCX were too small to allow diffusion of the deuterons through the system. The initial configurations and the modelling parameters are described below, together with the labels that will be used in subsequent discussion.

- A: $6 \times 6 \times 6$ repetition of the unit cell. O–D distance of 1.000 Å and a D–O–D bond angle of 109°. The initial O–O distances oblique and along the *c*-axis are unequal. Modelling used RMCXMOLS followed by RMCX.
- B: $6 \times 6 \times 6$ repetition of the unit cell. O–D distance of 1.000 Å and a D–O–D bond angle of 106°. The initial O–O distances oblique and along the *c*-axis are unequal. Modelling used RMCXMOLS followed by RMCX.
- C: $6 \times 6 \times 6$ repetition of the unit cell. O–D distance of 1.000 Å and a D–O–D bond angle of 106°. The initial O–O distances oblique and along the *c*-axis are unequal. Modelling used RMCXMOLS followed by RMCX. No rotation during RMCXMOLS.
- D: $6 \times 6 \times 6$ repetition of the unit cell. O–D distance of 1.000 Å and a D–O–D bond angle of 106°. The initial O–O distances oblique and along the *c*-axis are unequal. Modelling used RMCXMOLS followed by RMCX. Rotation only during RMCXMOLS.
- E: $10 \times 10 \times 10$ repetition of the unit cell. O–D distance of 1.000 Å and a D–O–D bond angle of 106°. The initial O–O distances oblique and along the *c*-axis are unequal. Modelling used RMCXMOLS followed by RMCX.
- F: $10 \times 10 \times 10$ repetition of the unit cell. O–D distance of 0.950 Å and a D–O–D bond angle of 106°. The initial O–O distances oblique and along the *c*-axis are unequal. Modelling used RMCXMOLS followed by RMCX.
- G: $10 \times 10 \times 10$ repetition of the unit cell. O–D distance of 1.000 Å and a D–O–D bond angle of 106°. The initial O–O distances oblique and along the *c*-axis are unequal. Modelling used RMCX only.
- H: $10 \times 10 \times 10$ repetition of the unit cell. O–D distance of 1.000 Å and a D–O–D bond angle of 106°. The initial O–O distances oblique and along the *c*-axis are equal. Modelling with RMCX only.
- I: $10 \times 10 \times 10$ repetition of the unit cell. O–D distance of 0.950 Å and a D–O–D bond angle of 106°. The initial O–O distances oblique and along the *c*-axis are unequal. Modelling with RMCX only.
- J: $6 \times 6 \times 6$ repetition of the unit cell. O–D distance of 1.000 Å and a D–O–D bond angle of 106°. The initial O–O distances oblique and along the *c*-axis are unequal. Modelling with RMCX only. Closest approaches used were the same as in paper I.
- K: $10 \times 10 \times 10$ repetition of the unit cell. O–D distance of 1.000 Å and a D–O–D bond angle of 106°. The initial O–O distances oblique and along the *c*-axis are unequal. Modelling with RMCX only. Closest approaches used were the same as in paper I.

A summary of the conditions and parameters used during RMC modelling is given in table 2.

Modelling took approximately 40 hours for RMCXMOLS followed by RMCX on a

Table 2. Summary of the conditions and parameters used during modelling. Column 1 gives the label of the configuration. Column 2 describes the number of unit cells in the Cartesian directions. Columns 3 and 4 give the initial O–D lengths and D–O–D angles respectively. Column 5 describes whether the O–O distances along and oblique to the *c*-axis are equal or unequal. Column 6 describes whether RMCXMOLS was used. The final column gives additional information relating to the modelling procedures.

Label	No of unit cells	Initial O–D	Initial D–O–D	O–O distance $\parallel$ and $\perp$ to c	Rigid mol. initially	Additional comments
A	6×6×6	1.00 Å	109°	unequal	Yes	
B	6×6×6	1.00 Å	106°	unequal	Yes	
C	6×6×6	1.00 Å	106°	unequal	Yes	No rigid mol.
D	6×6×6	1.00 Å	106°	unequal	Yes	Only rigid mol.
E	10×10×10	1.00 Å	106°	unequal	Yes	
F	10×10×10	0.95 Å	106°	unequal	Yes	
G	10×10×10	1.00 Å	106°	unequal	No	
H	10×10×10	1.00 Å	106°	equal	No	
I	10×10×10	0.95 Å	106°	unequal	No	
J	6×6×6	1.00 Å	106°	unequal	No	Cut-offs as I
K	10×10×10	1.00 Å	106°	unequal	No	Cut-offs as I

Table 3. Results obtained by the use of RMCXMOLS followed by RMCX on a $6 \times 6 \times 6$ repetition of the unit cell. Column 1 gives the various inter-atomic distances, angles and atomic mean square displacements (msds), for which the notation is given in figure 1. All other columns give the mean values of these quantities from the different models. The modelling conditions used for the different runs are described in the text. The results obtained after the use of RMCXMOLS and subsequently RMCX are presented under the headings MOLS and RMCX respectively. An underlined value denotes that it was fixed during modelling. All distances are given in Å, all angles are in degrees and all msds are in Å^2.

	A		B		C		D	
	MOLS	RMCX	MOLS	RMCX	MOLS	RMCX	MOLS	RMCX
O–O″	2.762	2.774	2.771	2.772	2.775	2.778	2.753	2.762
O–O′	2.772	2.738	2.729	2.735	2.762	2.729	2.746	2.743
O–D_2	1.000	1.009	1.000	1.009	1.000	1.011	1.000	1.033
O–D_1	1.000	1.003	1.000	1.009	1.000	1.010	1.000	1.033
O- -D_2''	1.855	1.851	1.882	1.877	1.816	1.815	1.879	1.871
O- -D_1'	1.845	1.852	1.877	1.877	1.824	1.824	1.888	1.878
D_2-D_3	1.632	1.641	1.597	1.603	1.597	1.602	1.597	1.622
D_2-D_2	1.632	1.641	1.597	1.605	1.597	1.608	1.597	1.627
D_2- -D_3''	2.329	2.331	2.350	2.350	2.325	2.329	2.351	2.357
D_2- -D_1'	2.364	2.345	2.389	2.390	2.348	2.349	2.404	2.408
O″–O–O″	108.9	108.9	108.9	108.9	108.7	108.8	109.47	109.2
O′–O–O″	109.7	109.6	109.7	109.7	109.8	109.9	109.47	109.5
D_2–O–D_3	109.47	109.2	106	105.5	106	105.5	106	104.1
D_2–O–D_1	109.47	109.4	106	105.8	106	105.3	106	104.4
O–D_2- -O″	156.8	155.4	152.6	152.0	167.5	164.9	151.8	149.2
O–D_1- -O′	154.6	153.4	151.4	150.2	158.1	155.9	152.4	148.6
O msd	0.0122	0.0147	0.0100	0.0125	0.0127	0.0158	0	0.0074
H msd	0.0292	0.0316	0.0262	0.0297	0.0195	0.0233	0.0259	0.0348

$6 \times 6 \times 6$ unit cell configuration, running on a digital DEC 3000 model 300X AXP work station. All fits give reasonable agreement with the data. This is illustrated in figures 2 and 3 which give the experimental data and corresponding fit for the $h\ 0\ l$ crystallographic plane. Some results are given in tables 3 to 6. In general no statistical error is given, because only one modelling run was performed. However in case G the error was obtained from consideration of eight different configurations. The results will be discussed in the following section.

Table 4. Results obtained by modelling $10 \times 10 \times 10$ repetitions of the unit cell. The modelling conditions used for the different runs are described in the text. Column 1 gives the various interatomic distances, angles and atomic mean square displacements (msds), for which the notation is given in figure 1. All other columns give the mean values of these quantities from the different models. The results obtained after the use of RMCXMOLS and subsequently RMCX are presented under the headings MOLS and RMCX respectively. An underlined value denotes that it was fixed during modelling. All distances are given in Å, all angles are in degrees and all msds are in $Å^2$.

	E		F		G	H	I
	MOLS	RMCX	MOLS	RMCX	RMCX	RMCX	RMCX
O–O″	2.758	2.757	2.754	2.754	2.758(1)	2.757	2.757
O–O′	2.758	2.761	2.763	2.763	2.746(1)	2.752	2.747
O–D_2	<u>1.000</u>	1.000	<u>0.950</u>	0.952	1.017(1)	1.017	0.971
O–D_1	<u>1.000</u>	1.000	<u>0.950</u>	0.953	1.014(1)	1.020	0.973
O- -D_2''	1.788	1.789	1.831	1.830	1.753(1)	1.752	1.799
O- -D_1'	1.812	1.789	1.864	1.863	1.743(1)	1.748	1.786
D_2-D_3	<u>1.597</u>	1.597	<u>1.517</u>	1.519	1.608(1)	1.609	1.533
D_2-D_2	<u>1.597</u>	1.599	<u>1.517</u>	1.521	1.608(2)	1.608	1.539
D_2- -D_3''	2.315	2.317	2.322	2.323	2.308(1)	2.309	2.318
D_2- -D_1'	2.336	2.336	2.344	2.344	2.302(1)	2.303	2.312
O″–O–O″	109.5	109.5	109.7	109.7	109.4(1)	109.5	109.4
O′–O–O″	109.2	109.3	109.0	109.1	109.4(1)	109.3	109.4
D_2–O–D_3	<u>106</u>	106.0	<u>106</u>	105.9	105.0(2)	104.7	104.8
D_2–O–D_1	<u>106</u>	106.1	<u>106</u>	105.9	105.1(2)	104.8	105.1
O–D_2- -O″	165.0	165.6	167.0	167.2	170.0(2)	169.2	169.9
O–D_1- -O′	152.9	156.4	153.2	156.1	169.9(2)	169.3	169.8
O msd	0.0065	0.0074	0.0052	0.0061	0.0039(7)	0.0051	0.0046
H msd	0.0138	0.0157	0.0103	0.0114	0.0101(8)	0.0101	0.0082

4. Discussion

The main aim of this work was to compare the results produced by reverse Monte Carlo with different modelling criteria, when applied to single-crystal neutron diffuse scattering over a large region of reciprocal space. The results of the original work, summarized in table 1 and discussed in detail in paper I, were inconsistent in some essentials with results obtained by more standard techniques. Here we will consider the results of the modelling runs described in the previous section, given in tables 3 to 6. It should be borne in mind that the results obtained by using RMC techniques are an instantaneous representation of the structure, rather than the average usually obtained by crystallography.

The fundamental difference between using RMCX and using RMCXMOLS followed by RMCX is that in the latter case the molecule is initially rigid, and hence bond lengths and angles are fixed during the initial part of the modelling. The effects of this were

Table 5. FWHM values in Å for the O–O″ distributions are given for various modelling runs.

Run	FWHM
A	0.38
B	0.39
C	0.35
D	0.35
E	0.18
F	0.20
G	0.16
H	0.21
I	0.16
J	0.25
K	0.18

Table 6. Results obtained by the use of RMCX only on a $6 \times 6 \times 6$ and a $10 \times 10 \times 10$ repetition of the unit cell. Column 1 gives the various inter-atomic distances, angles and atomic mean square displacements, for which the notation is given in figure 1. Columns 2 and 3 give their mean values. The modelling conditions used for the different runs are described in the text. All distances are given in Å, all angles in degrees and all msds are in $Å^2$.

	J	K
O–O″	2.7754	2.7572
O–O′	2.7159	2.7489
O–D_2	1.0169	1.0039
O–D_1	0.9781	1.0030
O- -D''_2	1.7876	1.7653
O- -D'_1	1.7636	1.7564
D_2-D_3	1.5912	1.5959
D_2-D_2	1.5843	1.5949
D_2- -D''_3	2.3188	2.3094
D_2- -D'_1	2.3124	2.3037
O″–O–O″	108.67	109.45
O′–O–O″	110.02	109.37
D_2–O–D_3	104.46	105.62
D_2–O–D_1	105.94	105.62
O–D_2- -O″	165.01	170.30
O–D_1- -O′	165.66	170.36
O msd	0.0124	0.0048
H msd	0.0165	0.0091

investigated by studying the changes in the resulting structure from having slightly different initial molecular geometries. When using RMCXMOLS followed by RMCX it is found that the value obtained for the average intra-molecular water angle is very dependent upon the fixed value of this angle during the RMCXMOLS fitting. This is clearly seen on comparing the D–O–D angles obtained in modelling run A, in which this angle was fixed at 109.47° initially, with all other cases. Similarly the O–D length is significantly altered in case F, where it was initially 0.95 Å, compared to case E, where it was initially 1.0 Å. Hence the choice of initial molecular geometry critically affects the resulting configuration if RMCXMOLS is used. However even if RMCX alone is used the final O–D length is influenced by the initial value. This explains the difference between the results from

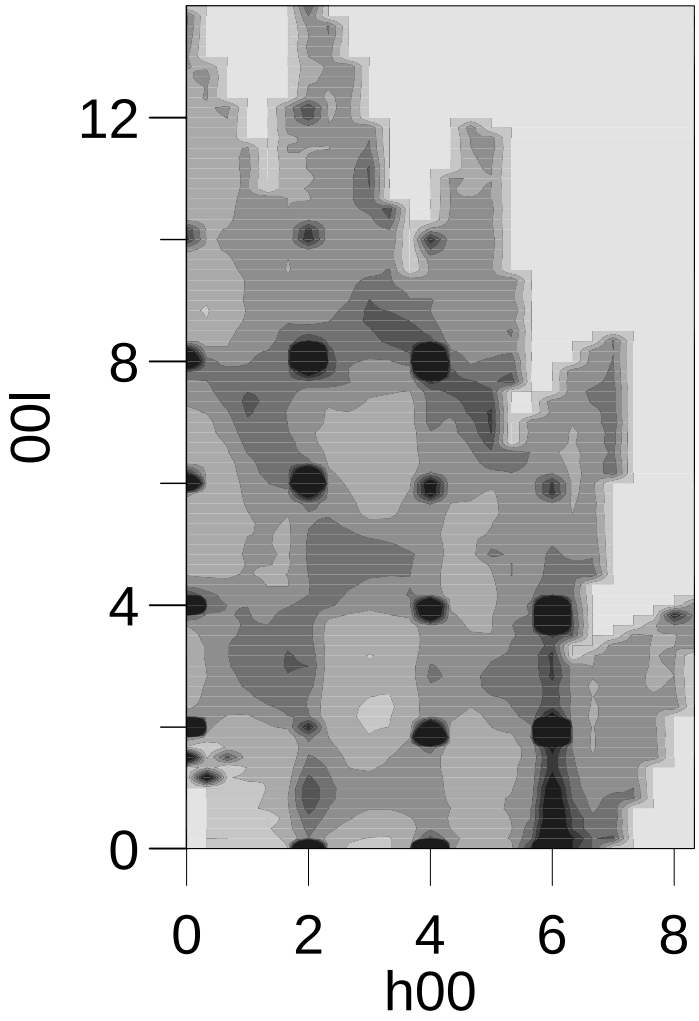

Figure 2. Experimental diffuse scattering in the $h\ 0\ l$ plane from D_2O ice Ih at 20 K. Darker shading corresponds to higher contour levels, which are the same as in figure 3.

paper I, runs G and H, and run I, where the initial O–D length was 0.975, 1.000 and 0.95 Å respectively. Hence when fitting to the ice diffuse scattering data of this study the initial molecular geometry has a significant effect on the results. This is exacerbated if RMCXMOLS is used initially.

RMC type techniques tend to maximize the amount of disorder, within the constraints applied, and so by keeping the molecule rigid during the early parts of modelling it was hoped that mean square displacements (msds) would be reduced from those found in paper I. If the deuterium mean square displacements are large, the O–D- -O angle is correspondingly small (i.e. a large mean square displacement leads to a large deviation from 180°). In paper I it was argued that the true average instantaneous value of this angle is about 170°, and is the same for both $O–D_1–O'$ and $O–D_2–O''$. The difference between the angle formed oblique and parallel to the *c*-axis is large in cases C, E and F. The reasons for this are not properly

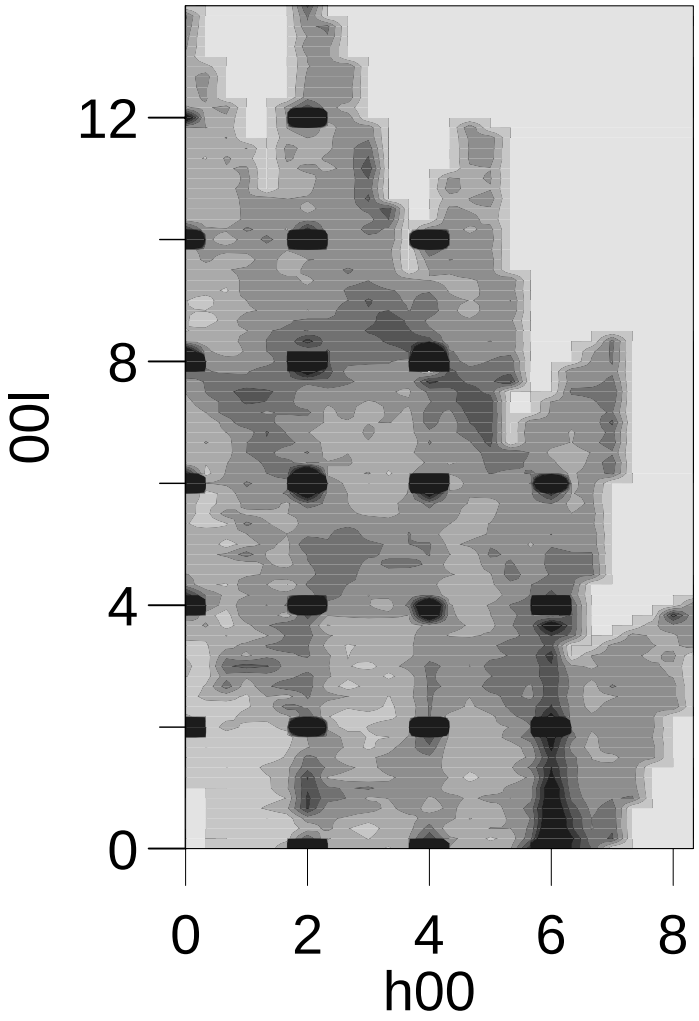

Figure 3. RMCXMOLS followed by RMCX fit to the scattering of figure 2 for configuration D.

understood. Excluding these from further consideration, in nearly all cases the average hydrogen bond angle is smaller than the expected 170°, corresponding to overly large mean square displacements. This is particularly true for A, B and D where the O- -D lengths are also correspondingly large. In fact the O–D- -O angle is largest in the original work of paper I and the present cases G, H and I, in all of which only RMCX was used. This shows that constraining the molecule in RMCXMOLS requires the structure to become unrealistic in order to improve the fit to the data. This leads to an increase rather than a decrease in the amount of disorder. If only rotational motions are allowed during RMCXMOLS (case D) the situation is even worse, with many of the resulting lengths and angles significantly altered. If only displacements are allowed during RMCXMOLS, case C, the amount of distortion is the same as in other RMCXMOLS cases.

The mean square displacements and bond-length distribution FWHMs are generally reduced by using a $10 \times 10 \times 10$ super-cell. In cases G to I the average O–D- -O angle

(just discussed) is close to 170°, the predicted 'correct' value (paper I). Using RMCX only on $10 \times 10 \times 10$ also gives other values more in accord with the crystallographic work of Kuhs and Lehmann (1986). For example the average O- -D bond-length of cases G, H and J is 1.75(1) Å which can be compared with the crystallographic value of 1.753(1) Å. The agreement in case I, where there was a different initial geometry, is not as good. The $10 \times 10 \times 10$ configurations similarly tend to decrease the difference between O–O′ and O–O″, again improving the agreement with the work of Kuhs and Lehmann (1986). This difference is also decreased in case H, where the two oxygen bond-lengths were initially the same. The O–O–O angles change in a corresponding manner.

In paper I the FWHM of the O–O distribution, in particular, was too broad, with the expected value of 0.049 Å from spectroscopic techniques (from Kuhs and Lehmann 1986, based on the work of Iorgansen and Rozenberg 1978). Table 5 shows the FWHM for the new models, and it can be seen that only in cases E to I, all of which are $10 \times 10 \times 10$ configurations, is it significantly reduced from the result of paper I.

The improvements obtained in moving to a $10 \times 10 \times 10$ configuration have two possible explanations, which cannot be readily decoupled. The first, and the most likely cause, is the finer binning of the data, which means the data averaging is over a smaller region of reciprocal space, and so its value is likely to be closer to the true value for the reciprocal lattice point at which the calculation is performed. This is especially important in regions where the diffuse scattering is changing rapidly with $\boldsymbol{Q}$. The second, the increased number of molecules, is likely to have had some effect, primarily because it improves the sampling of the static disorder, but this is believed by the authors to be less significant.

It was mentioned in section 2 that the closest approach distances in the present study were different from those in paper I. In the present study it was found that with larger O–D and D–D closest approach values the average O–D and D–D instantaneous values were generally increased, with consequent effects on other aspects of the local geometry. (Compare the results from J in table 6 with those from B in table 3; and from K in table 6 with G in table 4). The change this causes in $O–D_1$ is larger than that in $O–D_2$ for the $6 \times 6 \times 6$, hence these are equalized by using the larger closest approach values of the present study. With RMC studies it is usual to choose the closest approach values to give a smooth first peak in the pair correlation function $g(r)$, and figure 4 shows that this would lead to the use of the closest approach values of paper I. The choice of closest approach values is hence crucial in obtaining a physically realistic model and hence in the determination of accurate information from single-crystal diffuse scattering.

Constraints have been critically applied to the intra-molecular bond length distributions (Beverley and Nield 1997). However the results have shown that the final configurations are then even more strongly dependent upon the initial conditions.

5. Conclusions

The reverse Monte Carlo technique, RMCX, has been applied to single-crystal diffuse scattering data from ice, in order to carefully test the influence of different starting configurations and modelling criteria on the calculated structure. It has been found that the results depend on many things, including the initial molecular geometry and oxygen–oxygen bond-lengths, the size of the configuration and the closest approach values. The size of the configuration has two effects, one involving the improved statistics of the calculation and the second the $\boldsymbol{Q}$-resolution of the data. The RMCXMOLS technique, in which the molecules are initially kept rigid, was found to give results more strongly dependent on the initial geometry than RMCX, and hence its use is not sensible unless the molecular

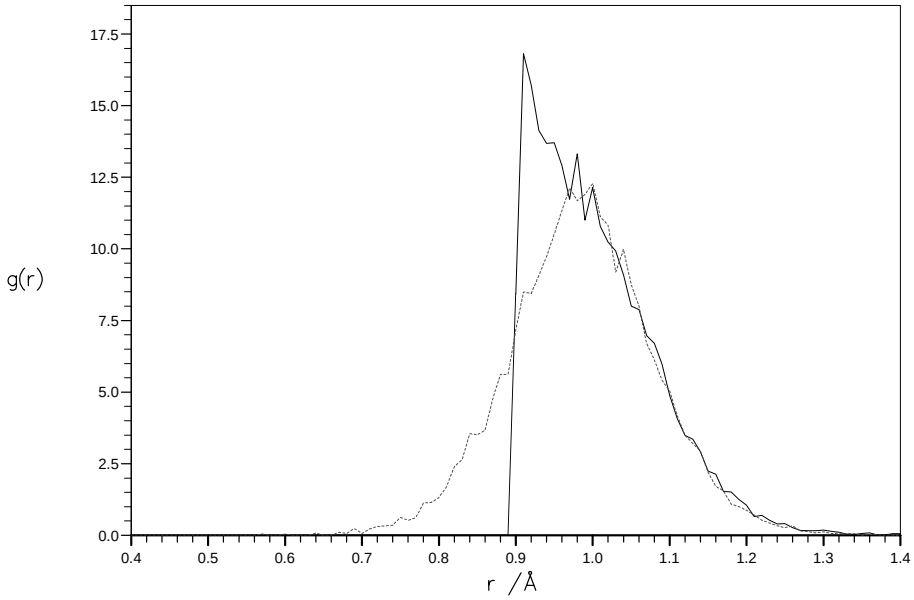

Figure 4. Plot of the first peak in the pair correlation function from $10 \times 10 \times 10$ configurations with different closest approaches. The dotted line is the $g(r)$ using the closest approaches of paper I, whereas the solid line is the $g(r)$ for the closest approaches used in this study.

parameters are known to a high degree of accuracy, and the molecule is truly inflexible. In response to these results, a new technique is under development allowing the molecule to be moved as an entity, but with significant flexibility. This is under test at present.

In conclusion, RMCX in its present form is not capable of extracting precise information on inter-atomic distances and angles from single-crystal diffuse scattering, because the results obtained are critically dependent on the modelling criteria. This is not specific to ice, and similar problems are likely to be encountered in all studies in which accurate interatomic parameters are required. Some of the problems can be alleviated by using as accurate an initial geometry as possible, and high-resolution data. The future of this technique rests in the development of simultaneous modelling of Bragg and diffuse scattering, which is presently being undertaken.

Acknowledgments

The authors wish to extend their gratitude to J-C Li for the measurement of the experimental data used in this study and to D A Keen, D K Ross and R W Whitworth for useful discussions. MNB wishes to acknowledge the Department of Employment for the award of an ESF traineeship and the Physics Laboratory at the University of Kent for financial support.

References

Bernal J D and Fowler R H 1933 *J. Chem. Phys.* **1** 515
Beverley M N and Nield V M 1997 *J. Phys. Chem.* at press
Iogansen A V and Rozenberg M Sh 1978 *Opt. Spektrosk.* **44** 87

Kuhs W F and Lehmann M S 1986 *Water Sci. Rev.* **2** 1
Li J C, Nield V M, Ross D K, Whitworth R W, Wilson C C and Keen D A 1994 *Phil. Mag.* B **69** 1173
McGreevy R L and Howe M A 1992 *Annu. Rev. Matter Sci.* **22** 217
McGreevy R L and Pusztai L 1988 *Mol. Simul.* **1** 359
Nield V M 1995 *Nucl. Instrum. Methods* A **354** 30
Nield V M, Keen D A and McGreevy R L 1995 *Acta Crystallogr.* A **51** 763
Nield V M and Whitworth R W 1995 *J. Phys.: Condens. Matter* **7** 259